Design of Multisensor Navigation System for Autonomous Precision Approach and Landing

*Ben K.H. Soon[1], Steve Scheding[1], Hyung-Keun Lee[2] and Hung-Kyu Lee[3]

[1]ARC Centre of Excellence for Autonomous Systems (CAS),
Australian Centre for Field Robotics (ACFR), University of Sydney
(E-mail: b.soon@acfr.usyd.edu.au / skahhol@dso.org.sg, s.scheding@acfr.usyd.edu.au)
[2]School of Electronics, Telecommunication and Computer Engineering, Hankuk Aviation University.
(E-mail: hyknlee@hau.ac.kr)
[3]Department of Civil Engineering, Changwon National University. (E-mail: hkyulee@changwon.ac.kr)

Abstract

Precision approach and landing of aircraft in a remote landing zone autonomously present several challenges. Firstly, the exact location, orientation and elevation of the landing zone are not always known; secondly, the accuracy of the navigation solution is not always sufficient for this type of precision maneuver if there is no DGPS availability within close proximity. This paper explores an alternative approach for estimating the navigation parameters of the aircraft to the landing area using only time-differenced GPS carrier phase measurement and range measurements from a vision system. Distinct ground landmarks are marked before the landing zone. The positions of these landmarks are extracted from the vision system then the ranges relative to these locations are used as measurements for the extended Kalman filter (EKF) in addition to the precise time-differenced GPS carrier phase measurements. The performance of this navigation algorithm is demonstrated using simulation.

Keywords: Inertial, GPS, vision, tightly-coupled, precision approach and landing.

1. Introduction

With full GPS operational capability declared in the mid-1990s, research has been ongoing in the development of a local area augmentation system to provide an all-weather approach, landing and surface navigation capability, that can fulfill the Required Navigation Performance (RNP) parameters (accuracy, availability, integrity and continuity) for CAT I/II/III aircraft precision approach and landing, as a replacement for the Instrument Landing System (ILS) and Microwave Landing System (MLS). Standalone GPS and conventional code-phase differential GPS are unable to meet the stringent navigation requirements in most airborne applications, because the performance of satellite-based navigation systems are dependent on both the number and geometric distribution of satellites tracked by the receivers. Due to the limited number of GPS satellites, a sufficient number of visible satellites cannot be guaranteed everywhere, 24 hours a day. Even in situations when some low elevation satellites can be tracked, the measurements from these satellites are contaminated by relatively high atmospheric noise. Though greater satellite visibility can be expected with the development of Galileo by the European Commission (EC) and European Space Agency (ESA) and new funding for the restoration of the Russian GLONASS announced by the Russian Federation, the intrinsic shortcoming of satellite-based positioning systems results in poor accuracy in the vertical component, which is typically about three times worse than that of the horizontal components.

Studies have shown that some means of augmentation can address these drawbacks in order to meet the specified requirements. Airport pseudolites have been suggested as an alternative to satisfy the stringent performance requirements of CAT I/II/III approach systems. Airport pseudolites are ground-based transmitters which emit GPS-like signals; that enhances GPS navigation by providing increased accuracy, availability and integrity. Navigation accuracy improvement can occur due to better local geometry, as measured by a lower vertical dilution of precision (VDOP), which is crucial in aircraft precision approach and landing applications. Accuracy and integrity enhancement can also be achieved by using an airport pseudolite's integral data link to support differential modes of operation and timely transmission of integrity warning information. Availability is increased because airport pseudolites provide additional ranging sources to augment the GPS constellation. Flight trials have been conducted as a joint project between DSO National Laboratories, Singapore and Satellite Navigation And Positioning (SNAP), The University of New South Wales, Australia. Results demonstrated the effectiveness of an integrated carrier-smoothed differential GPS/pseudolite system which is able to achieve sub-meter accuracies both laterally and vertically [1] [2].

The use of airport pseudolites offers many potentially benefits for GPS airborne applications. However, there are a number of technical issues, which must be addressed. Some of the main issues are ground multipath, and the 'near-far' problem where large power level variation is expected over the final approach path. More importantly, the number and the geometric distribution of the airport pseudolites on the ground will also have a significant impact on the performance of an augmented system. The overall performance can be affected in terms of the positioning accuracy, integrity and reliability of the ambiguity resolution. Multipath is also expected to be the largest error source for the ground reference station [14].

This paper describes an alternative design of a multisensor navigation system for precision approach and landing consists of an integrated tactical-grade ($<10^{\circ}$/h) inertial navigation system (INS), Global Positioning System (GPS) and a vision system, as seen in Figure 1 the multisensor navigation system configuration. The raw measurements from the standalone GPS and vision system are the time-differenced GPS carrier-phase measurements

and relative range measurements to the ground landmarks respectively. The processing of velocity measurements using time difference carrier phase provides an increase in velocity accuracy of the navigation solution which leads to increase in attitude accuracy but lacks in state observability in position estimates and relative information to remote landing zone. Distinct ground landmarks are marked before the landing zone. The positions of these landmarks are extracted from the vision system then the ranges relative to these locations are used as measurements. For the vision system in this case it is assumed to be able to provide 3 dimensional positions of the ground landmarks (e.g., radar, LIDAR or stereo vision) and provides range measurements. A centralized filtering strategy is used by fusing the raw sensor measurements from all the navigation sensors. Usually DGPS corrections are required in order to exploit the high accuracy of the carrier phase measurements by removing the common mode errors like atmospheric errors, satellite ephemeris and clock errors. Techniques like carrier smoothed differential code or ambiguity resolution can be applied and result in positioning accuracy in the order of centimeter or better. However in this paper, the technique proposed does not necessitate differential GPS corrections or raw measurements being transmitted from a base station. To evaluate the performance of the multisensor navigation system for approach and landing, simulations are conducted according to 3 different scenarios: carrier-smooth code-differential GPS/INS, the proposed integrated GPS/INS/vision system and INS aided with standalone GPS measurements are performed.

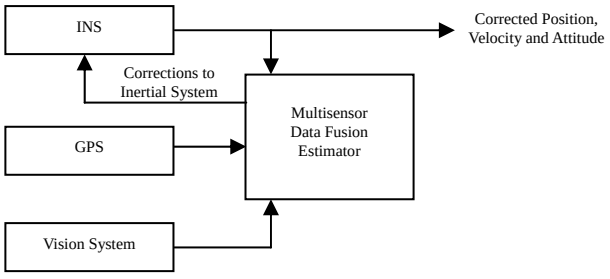

Figure1. Indirect Feedback Multisensor Navigation Configuration

2. Integration Architectures

The types of system integration are characterized in two ways: by the extent to which data from each component aids the other's function, that is, by the mechanization or the architecture of the system; and by the method of combining or fusing the data to estimate navigation solution. Although, to some extent, the method of data blending actually reflects the mechanization imposed by the hardware configuration, different levels of processing may be applied to a particular mechanization. In fact, clear distinctions between mechanizations and methods of data processing fade as the system integration becomes tighter.

More descriptively, the mechanization is referred to as a coupling, where no coupling (uncoupled integration) implies no data feedback from either instrument to the other for the purpose of improving its performance; and, in tight coupling the sensors are treated as belonging to a single system producing several complementary types of data that are processed simultaneously and optimally and used to enhance the function of individual sensor components where possible. Tightly coupled systems combine unprocessed measurements from the sensors through a single estimator. In a loosely coupled system processed data from one instrument are fed back in an aiding capacity to improve the utility of the other's performance, but each instrument still has its own individual data processing algorithm. Loosely coupled systems are also known as a filter-aided-filter where processed measurements are then combined through another estimator to obtain a final estimated navigation solution.

3. Velocity Estimation Using Differences of Carrier-Phase Measurements

The velocity vector can be extracted from the GPS measurements in two methods. The first option is using the Doppler raw measurement, which provides directly the radial velocity from Phase Lock Loop (PLL) and the second method uses a basic form of the carrier phase measurements difference between two epochs. It is known that the phase velocity estimation is more accurate than Doppler observations [3]. In the following section a method is presented, which allows to increase the performance of tightly-coupled systems by using carrier phase measurements instead of delta-range measurements to aid the INS.

3.1 Carrier Phase Measurements

A measurement much more precise than that of a code phase is the phase of the carrier received from a satellite. The carrier phase measurement is the difference between the phases of the receiver-generated carrier signal and the carrier received from a satellite at the instant of the measurement. The phase of the received signal at any instant can be related to the phase at the satellite at the time of transmission in terms of the transit time of the signal. The carrier phase measurement is this thus an indirect and an ambiguous measurement of the signal transit time.

The measurement model of a carrier phase measurement can be written as

$$\phi = \lambda^{-1}[r - I_\phi + T_\phi] + \frac{c}{\lambda}(\delta t_u - \delta t_s) + N + \varepsilon_\phi \qquad (1)$$

where ϕ is the measured carrier phase in cycles; r is the geometric range between the user position and the satellite position; λ is the wavelength; c is the speed of light; I_ϕ is the ionospheric error; T_ϕ is the tropospheric error; δt_u is the user clock error; δt_s is the satellite clock error; N is the integer ambiguity and ε_ϕ is the unmodelled effects, modeling error and measurement error.

3.2 Time-Differenced Carrier Phase Measurements

Carrier phase measurements are encumbered with integer ambiguities which have to be resolved before the measurements can be used for precise positioning and navigation. The integers remain fixed as long as the carrier tracking loop maintains lock. Momentary loss of phase lock can result in a discontinuity in the integer cycle count even though the fractional part of the phase is measured continuously.

Operations using carrier phase processing for accurate estimation in general carry a burden of resolving and maintaining cycle counts. Without that cycle count information, position estimates are ambiguous; in error by an unknown integral number - potentially a very large number - of wavelengths. In real-time kinematic (RTK) mode, the measurements at the reference station are transmitted to the rover on a communication link. A

key feature required by RTK is the ability to estimate the integer ambiguities while the rover is in motion and common mode errors are removed by using measurements from the base station. Integer resolution techniques, while clever and often successful, carry disadvantages that can seriously compromise overall success. Potential problems include delays that can disrupt real-time operation because the general RTK technique for solving for the correct ambiguity is to search the uncertainty region for the correct solution using error minimization techniques. This requires a minimum amount of geometry change between the user and the satellites. The amount of change required depends upon the initial uncertainty, which is usually that of the double-differenced pseudorange measurement solutions [7]. Further problems can arise from temporary false indications of ambiguity resolution, producing errors far beyond acceptable design limits [6].

Triple differenced carrier phase measurements are already used in many applications, for estimation of GPS velocity which is independent of ambiguity terms [11] and mostly for detection of cycle slips. Triple differenced measurements are obtained by first forming differences between the measurements of a base station and a rover, second between different satellites and finally between two successive epochs. With the approach described here, only differences between two successive carrier phase measurements at t_k and t_{k-1}, respectively are formed and a reference station is not required. Such a time differenced carrier phase measurement (in cycles) can be formulated as follows:

$$\begin{aligned}\Delta\phi &= \phi_{t_k} - \phi_{t_{k-1}} \\ &= [\lambda^{-1}[r - I_\phi + T_\phi] + \frac{c}{\lambda}(\delta t_U - \delta t_S) + N + \varepsilon_\phi]_{t_k} - \\ &\quad [\lambda^{-1}[r - I_\phi + T_\phi] + \frac{c}{\lambda}(\delta t_U - \delta t_S) + N + \varepsilon_\phi]_{t_{k-1}} \\ &= r_{t_k} - r_{t_{k-1}} + \delta t_{Ut_k} - \delta t_{Ut_{k-1}} + \varepsilon_{\Delta\phi} \\ &= \lambda^{-1}\Delta r + \frac{c}{\lambda}\delta\dot{t}_U + \varepsilon_{\Delta\phi}\end{aligned} \tag{2}$$

where Δr is change in range between two measurement epochs; $\delta\dot{t}_U$ is the user clock drifts and the remaining measurement error that is not removed by forming time differences is denoted with $\varepsilon_{\Delta\phi}$ which is the combined error due to changes in the satellite clock, ionospheric and tropospheric. Using time difference of the carrier phase measurements from two consecutive epochs eliminates the integer ambiguity, N and common mode errors allowing direct estimation of precise velocity. The constant integer phase ambiguity is removed completely and an estimation of this quantity using techniques like RTK is not necessary.

A model for change in range, Δr between two consecutive epochs can be approximated by

$$\begin{aligned}\Delta r &= \boldsymbol{l}_{t_k}.(\boldsymbol{x}_{S\,t_k} - \boldsymbol{x}_{U\,t_k}) - \boldsymbol{l}_{t_{k-1}}.(\boldsymbol{x}_{S\,t_{k-1}} - \boldsymbol{x}_{U\,t_{k-1}}) && \text{(3a)} \\ &\approx \boldsymbol{l}_{t_k}.[(\boldsymbol{x}_{S\,t_k} - \boldsymbol{x}_{U\,t_k}) - (\boldsymbol{x}_{S\,t_{k-1}} - \boldsymbol{x}_{U\,t_{k-1}})] \\ &= \boldsymbol{l}_{t_k}.(\boldsymbol{v}_S - \boldsymbol{v}_U) && \text{(3b)}\end{aligned}$$

where $\boldsymbol{v}_S$ is the satellite velocity vector, known from the navigation message broadcast by the satellite; $\boldsymbol{v}_U$ is the user velocity vector, to be estimated. The user-to-satellite line-of-sight unit vector $\boldsymbol{l}_{t_k}$ at time t_k is determined from an estimate of the user position.

Substituting Eq. (3) into Eq. (2) leads to a time differenced carrier phase measurement (in meters)

$$\Delta\phi = \boldsymbol{l}_{t_k}.(\boldsymbol{v}_S - \boldsymbol{v}_U) + \delta\dot{t}_U + \varepsilon_{\Delta\phi} \tag{4}$$

The carrier-phase derived Doppler can be obtained using different techniques: differencing carrier phase measurements in the time domain, normalizing them with the time interval of the differenced measurements, Eq. (2), by fitting a curve using polynomials of various orders with successive phase measurements, or using first order central difference approximation of the carrier phase rate [10].

4. Extended Kalman Filter Design Description

This section presents the filter model propagation and measurement models. The following presentation will be divided up by navigation subsystems; first the INS portion of the model will be presented then the GPS. In this paper, a tightly coupled GPS/INS/Vision system is realized using a 17-state extended Kalman filter where the error state is given by

$$\boldsymbol{\delta x_k} = [\boldsymbol{\delta r} \quad \boldsymbol{\delta v} \quad \boldsymbol{\psi} \quad \boldsymbol{\delta f_b} \quad \boldsymbol{\delta\omega_b} \quad \delta t_{u_b}\, \delta t_{u_d}]^T \tag{5}$$

where $\boldsymbol{\delta r}$, $\boldsymbol{\delta v}$ and $\boldsymbol{\psi}$ are the general INS error states of positions, velocities and attitudes whereas $\boldsymbol{\delta f_b}$ and $\boldsymbol{\delta\omega_b}$ are the accelerometer and gyroscope bias respectively modeled as a first-order Gauss Markov processes; δt_{u_b} and δt_{u_d} are the GPS receiver clock bias and drift error states.

4.1 INS Error Model

Various form of INS error models have been developed, however all these models can be derived using a unified approach, and considered equivalent. The ψ-angle error model is obtained from a linear perturbation analysis of the strapdown inertial navigation errors in the navigation frame (*n-frame*), which is the navigation frame maintained by the inertial navigation system. The computer frame is a "known" reference frame, hence perturbations of the computer frame angular position and angular rate are zero. This leads to a simpler model than the φ-angle error model. The INS error model used in this paper is based on the *Psi*-angle approach developed by [8] [13]:

$$\boldsymbol{\delta\dot{r}_e^n} = \boldsymbol{\delta v_e^n} - \boldsymbol{\omega_{en}^n} \times \boldsymbol{\delta r_e^n} \tag{6}$$

$$\boldsymbol{\delta\dot{v}_e^n} = -(\boldsymbol{\omega_{in}^n} + \boldsymbol{\omega_{ie}^n}) \times \boldsymbol{\delta v_e^n} + \nabla - \boldsymbol{\psi^n} \times \boldsymbol{f^n} + \boldsymbol{\delta g} \tag{7}$$

$$\boldsymbol{\dot{\psi}^n} = -\boldsymbol{\omega_{in}^n} \times \boldsymbol{\psi^n} + \boldsymbol{\varepsilon} \tag{8}$$

where $\boldsymbol{\delta v}$, $\boldsymbol{\delta r}$ and $\boldsymbol{\psi}$ are the velocity, position and attitude error vectors respectively; ∇, the accelerometer error vector; $\delta\boldsymbol{g}$, the error in the computed gravity vector; $\boldsymbol{\varepsilon}$, the gyro drift vector; $\boldsymbol{\omega_{en}^n}$, the angular rate of the *n-frame* with respect to the earth; $\boldsymbol{\omega_{ie}^n}$, the angular rate of the earth with respect to inertial space and $\boldsymbol{\omega_{in}^n} = \boldsymbol{\omega_{ie}^n} + \boldsymbol{\omega_{en}^n}$, the angular rate of the *n-frame* with respect to the inertial space.

The dynamic matrix is represented as:

$$\begin{bmatrix} \dot{\delta r}_e^n \\ \dot{\delta v}_e^n \\ \dot{\psi} \\ \dot{\delta f}_b \\ \dot{\delta \omega}_b \end{bmatrix} = \begin{bmatrix} (-\omega_{en}^n \times) & I & 0 & 0 & 0 \\ F_{21} & (-(\omega_{in}^n + \omega_{ie}^n)\times) & (f_b^n \times) & C_b^n & 0 \\ 0 & 0 & (-\omega_{in}^n \times) & 0 & -C_b^n \\ 0 & 0 & 0 & F_{44} & 0 \\ 0 & 0 & 0 & 0 & F_{55} \end{bmatrix} \begin{bmatrix} \delta r_e^n \\ \delta v_e^n \\ \psi \\ \delta f_b \\ \delta \omega_b \end{bmatrix} + \begin{bmatrix} 0 & 0 & 0 & 0 \\ C_b^n & 0 & 0 & 0 \\ 0 & -C_b^n & 0 & 0 \\ 0 & 0 & I & 0 \\ 0 & 0 & 0 & I \end{bmatrix} \begin{bmatrix} w_\nabla \\ w_\varepsilon \\ w_{\nabla_b} \\ w_{\varepsilon_b} \end{bmatrix} \tag{9}$$

where the sub-matrices are expressed as:

$$F_{21} = diag[-g/R_e \quad -g/R_e \quad 2g/R_e]$$
$$F_{44} = diag[-\tau_{\nabla_{b_x}} \quad -\tau_{\nabla_{b_y}} \quad -\tau_{\nabla_{b_z}}]$$
$$F_{55} = diag[-\tau_{\varepsilon_{b_x}} \quad -\tau_{\varepsilon_{b_y}} \quad -\tau_{\varepsilon_{b_z}}]$$

where R_e is the Earth radius plus vehicle altitude; τ_{∇_b} and τ_{ε_b} are the time-constants for the first-order Gauss Markov processes of the accelerometer and gyroscope bias respectively and $w = [w_\nabla \quad w_\varepsilon \quad w_{\nabla_b} \quad w_{\varepsilon_b}]^T$ are all zero-mean Gaussian white noise vectors.

4.2 GPS Receiver Clock Error Model

A basic 2-state model is commonly used in most Kalman filter implementations allows for the estimation of both clock bias and drift, representing the dominant error source associated with the GPS measurements. Numerical values for the spectral densities of the white noise forcing functions depend on the quality of the crystal clock. Besides the receiver clock error model, filter designers have also been concerned with the errors in the pseudorange and carrier phase measurements to each satellite due to residual satellite clock and orbit errors, transmission path effects (atmospheric errors) and tracking loop errors. Inclusion of an error state for each of these measurements can obtain a calibration of the measurement under certain conditions.

The differential clock model is [5]:

$$\begin{bmatrix} \dot{\delta t}_{U_b} \\ \dot{\delta t}_{U_d} \end{bmatrix} = \begin{bmatrix} 0 & 1 \\ 0 & 0 \end{bmatrix} \begin{bmatrix} \delta t_{U_b} \\ \delta t_{U_d} \end{bmatrix} + \begin{bmatrix} w_{U_b} \\ w_{U_d} \end{bmatrix} \tag{10}$$

4.3 Measurement Model

The observation model of the filter is based on two types of measurements. The first is the velocity measurement determined by GPS phase rate and the second is the range measurement relative to the ground landmarks.

Time-Differenced GPS Carrier Phase Measurement Model

There are two approaches to derive the difference measurement. Using Eq. (3b), which is a direct processing approach used in this paper to derive the range rate difference measurement. The measurement is formulated by estimating an INS range rate measurement using INS positions and velocities and the ephemeris provided satellite positions and velocities and subtracted by the time difference GPS carrier phase measurement. The INS range-rate, Δr_{INS} is derived as follows,

$$\Delta r_{INS} = \boldsymbol{l}_{INS\,t_k} . (\boldsymbol{v}_s^n - \boldsymbol{v}_{INS}^n) \tag{11}$$

where $\boldsymbol{v}_s^n = [v_{x_s} \quad v_{y_s} \quad v_{z_s}]^T$ and $\boldsymbol{v}_{INS}^n = [v_{x_{INS}} \quad v_{y_{INS}} \quad v_{z_{INS}}]^T$ are the satellite velocities and INS velocities in the *n-frame* respectively and $\boldsymbol{l}_{INS\,t_k}$ is user-to-satellite line-of-sight unit vector at time t_k determined from an estimate of the INS position. Since the INS calculated range rate is a nonlinear function of the INS and GPS satellite positions and velocities, a truncated first order Taylor series is performed to linearize Eq. (10) for use in the EKF. Linearizing the INS range rate also reformats it in terms of the error states needed in the error model for the EKF. Evaluating the Taylor expansion about the INS velocities, $\boldsymbol{v}_{INS}^n$ as:

$$\Delta r_{INS} = \Delta r\big|_{x_{INS}^n, v_{INS}^n} - \boldsymbol{l}_{INS\,t_k} . \boldsymbol{\delta v}_{INS}^n \tag{12}$$

where the INS velocity error vector, $\boldsymbol{\delta v}_{INS}^n = \boldsymbol{\delta v}_e^n$. The difference range rate measurement at time t_k is provided by subtracting Eq. (12) from Eq. (4),

$$\begin{aligned} \delta z_{\Delta r_{INS}} &= \Delta r_{INS} - \Delta\phi \\ &= -\boldsymbol{l}_{INS\,t_k} . \boldsymbol{\delta v}_{INS}^n - \dot{\delta t}_U + \varepsilon_{\Delta\phi} \\ &= -\boldsymbol{l}_{INS\,t_k} . \boldsymbol{\delta v}_e^n - \dot{\delta t}_U + \varepsilon_{\Delta\phi} \end{aligned} \tag{13}$$

Another approach to process the difference measurement is by using a delayed state Kalman filter [4] [5]. However, there are several disadvantages using the delayed state Kalman filter: For the covariance matrix of the measurement noise of all carrier phase differences available at the current epoch has diagonal form. Using a delayed state Kalman filter, this diagonal form is lost. Therefore, a sequential, scalar processing of these measurements which is desirable because of numerical reasons is not possible without an additional decorrelation procedure [12]. This result in a further increase in computational load, besides the already increased computational load due to the usage of a delayed state Kalman filters itself. Two alternative delayed-state Kalman filter were proposed in [6] [12].

Range Measurement Model

For each ground landmarks being tracked by the vision system, there is a relative range measurement updates to the filter. These measurement updates are again difference measurements formed by taking the difference of the INS estimated range to landmark and the range measurement from the vision system.

The range measurement is defined as $r_{LANDMARK}$, the range from the aircraft to landmark and ε_r, vision measurement noise:

$$r_{VISION} = r_{LANDMARK} + \varepsilon_r \tag{14}$$

With the ground landmark positions predetermined by the aircraft while approaching the runway, the INS estimated range to landmark is defined as:

$$r_{INS} = \boldsymbol{l}_{LANDMARK\text{-}INS\,t_k} . (\boldsymbol{x}_{LANDMARK}^n - \boldsymbol{x}_{INS}^n) \tag{15}$$

where $\boldsymbol{x}^n_{LANDMARK} = [x_{LANDMARK} \quad y_{LANDMARK} \quad z_{LANDMARK}]^T$ and $\boldsymbol{x}^n_{INS} = [x_{INS} \quad y_{INS} \quad z_{INS}]^T$ are the landmark and INS position in the *n-frame* respectively and $\boldsymbol{1}_{LANDMARK\text{-}INS\,t_k}$ is user-to-landmark line-of-sight unit vector at time t_k as determined from an estimate of the INS position. Since this equation is nonlinear, a Taylor series expansion is performed to generate the first order linear equation on terms of the INS position error states

$$r_{INS} = r\big|_{x^n_{INS}} - \boldsymbol{1}_{LANDMARK\text{-}INS\,t_k}.\boldsymbol{\delta x}^n_{INS} \tag{16}$$

and subtracting Eq. (16) from Eq. (14) to form the range difference measurement to each landmark:

$$\begin{aligned} \delta z_{r_{INS}} &= -\boldsymbol{1}_{LANDMARK\text{-}INS\,t_k}.\boldsymbol{\delta x}^n_{INS} + \varepsilon_r \\ &= -\boldsymbol{1}_{LANDMARK\text{-}INS\,t_k}.\boldsymbol{\delta r}^n_e + \varepsilon_r \end{aligned} \tag{17}$$

5. Simulation and Results

To investigate the performance of the tightly coupled GPS/INS/vision system, simulations are conducted according to the following three scenarios:

- Scenario I - the traditional carrier-smoothed code-differential GPS/INS navigation system [15];
- Scenario II - the proposed GPS/INS/vision system with 3 unknown ground landmarks placed before the landing zone since at least 3 range measurements are required to estimate the aircraft positions.
- Scenario III – the standalone GPS-aided INS system using carrier-smoothed GPS pseudorange measurements.

The nominal flight trajectory in the simulations is approximately a straight path to the North aligned to the landing zone starting at an altitude of 300 meters, at a constant velocity of 20 m/s, with a glide slope of 5^o and flight duration of 200 s. The profile of the aircraft landing trajectory is shown in Fig. 2. For the Scenario II simulation, it is assumed that the ground landmarks are within operating range and field of view of the vision system for a duration 20 s during the approach (between time interval 150s to 170s). After that the navigation system switched back to using only time-difference carrier-phase measurements as updates and the time from the last vision measurement update to touchdown as within 30 s. The update rate for the IMU measurements is simulated at 100 Hz whereas for the raw GPS and range relative to landmarks measurements are updated at 1 Hz.

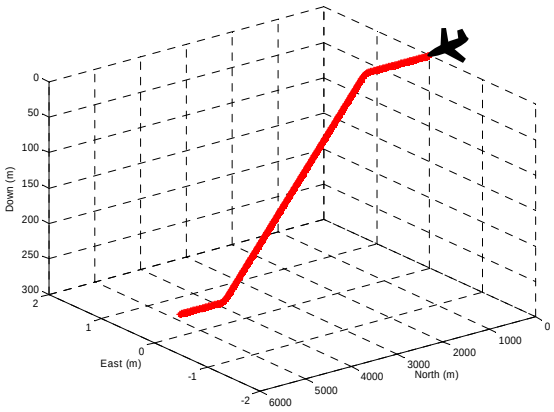

Figure 2 Simulated Flight Trajectory.

Fig. 3, 4 and 5 show the positional errors from the carrier-smoothed code-differential GPS/INS system, the tightly-coupled GPS/INS/vision system and standalone GPS-aided INS system as calculated by the difference between the estimated and reference positional data obtained in the simulation. Fig. 4 shows that the simulated system performance is comparable to the carrier-smoothed code-differential GPS/INS system and it is able to track the trajectory sufficiently well to support landing at the desired landing zone with 3D positional accuracies within 0.5 m from the time the landmarks are within the operating range of the vision sensor till end of simulation. Within the period when relative range measurements are available there is an improvement in the positional accuracies due to changing geometry between the aircraft and landmarks. Actually the proposed concept is useful even if the absolute positions of the landmarks are not known exactly. Consider the case where the landmarks have unknown error in its position estimate. Clearly, the aircraft navigation solution is computed based on the measurements to these landmarks. The subsequent error in the aircraft's estimated position would be approximately the same as the error in the landmark positions. The relative position vectors between the aircraft and landmarks would be unaffected. In other words, the aircraft estimated position is relative to the positions ascribed to the landmarks.

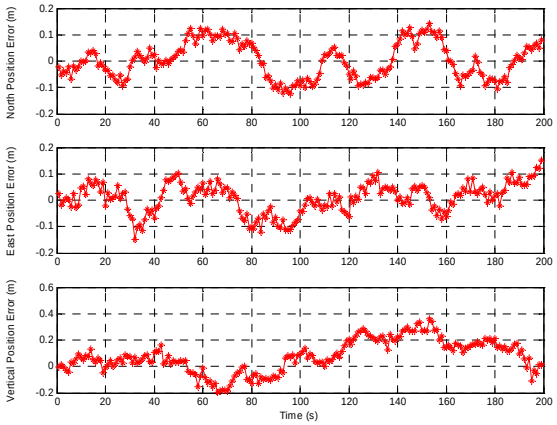

Figure 3 Tightly-Coupled Carrier-Smoothed Code-Differential GPS/INS Position Error Estimates

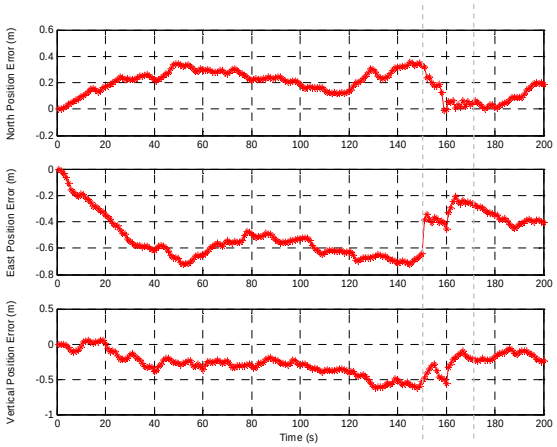

Figure 4 Tightly-Coupled GPS/INS/Vision Position Error Estimates

Fig. 5 shows the performance of a standalone GPS-aided INS system using carrier-smoothed GPS pseudorange measurements as updates. It is apparent that it is unable to meet the navigation requirements for an aircraft to perform precision approach and

landing. Even though with good GPS satellite geometry towards the end of the approach, the vertical positional error is about 20 m.

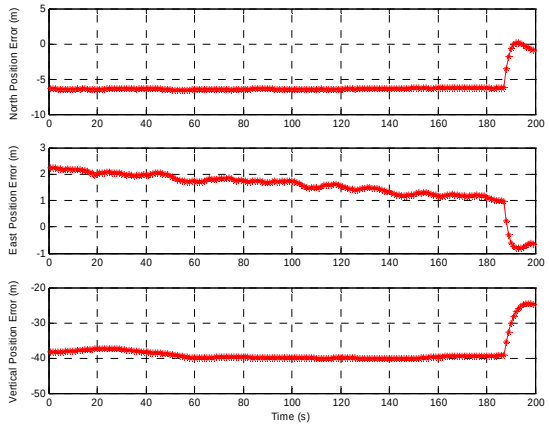

Figure 5 Standalone GPS-aided INS Position Error Estimates

6. Conclusion

In this paper, the processing of time-differenced carrier-phase measurements and range measurements relative to distinct ground landmarks was proposed for a tightly-coupled GPS/INS/vision system. Instead of the traditional precision approach and landing which exploit carrier phase measurements, differential corrections from a reference and resolving of integer ambiguities are not required. The approach proposed in this paper has been presented as an alternative simple solution for landing aircraft autonomously in remote landing zones.

This topic has by no means been completely explored. Future work will involve exploring the possibility of using INS/*p*SLAM (*pseudo* Simultaneous Localisation And Mapping) concept and apply it on both land and air platforms.

Reference

1. B.K.H. Soon, E.K. Poh, J. Barnes, J. Zhang, H.K. Lee, H.K. Lee and C. Rizos, “Flight Test Results of Precision Approach and Landing Augmented by Airport Pseudolites”, *16th International Technical Meeting of the Satellite Division of The Institute of Navigation*, 9-12 September 2003, Portland, Oregon,

2. B.K.H. Soon, E.K. Poh, J. Barnes, H.K. Lee, J. Zhang, C. Rizos and H.K. Lee, “Real-Time Flight Test Results of an Integrated GPS/Pseudolite Autolanding System”, *European Navigation Conference GNSS 2004*, 16-19 May 2004, Rotterdam, The Netherlands.

3. J. Hebert, J. Keith, S. Ryan, M. Szannes, G. Lachapelle and M.E. Cannon, “DGPS Kinematic Phase Signal Simulation Analysis for Precise Aircraft Velocity Determination”, *ION Annual Meeting*, 3 June – 2 July 1997, Albuquerque, NM

4. R.G. Brown and L.L. Hagerman, “An Optimum Inertial/Doppler-Satellite Navigation System”, *Navigation: Journal of The Institute of Navigation,* Vol. 16, No. 3, Fall 1969.

5. R.G. Brown and P.Y.C. Hwang, *Introduction to Random Signals and Applied Kalman Filtering*, 3rd Edition, New York: J, Wiley and Sons, Inc., 1997.

6. J.L. Farrell, “Carrier Phase Processing Without Integers”, *ION 57th Annual Meeting/CIGTF 20th Biennial Guidance Test Symposium*, Albuquerque, NM, 11-13 June 2001.

7. M. Kayton and W.R. Fried, Avionics Navigation Systems. 2nd Edition, J, Wiley and Sons, Inc., 1997.

8. I.Y. Bar-Itzhack and N. Berman, “Control Theoretic Approach to Inertial Navigation Systems”, *AIAA Journal of Guidance, Control and Dynamics*, Vol. 11, No. 3, 1988.

9. R.A. Gray and P.S. Maybeck, “An Integrated GPS/INS/Baro and Radar Altimeter System for Aircraft Precision Approach Landings**”,** *Proceedings of the IEEE 1995 National Aerospace and Electronics Conference, NAECON 1995*, Vol. 1, 22-26 May 1995

10. M. Szarmes, S. Ryan, G. Lachapelle and P. Fenton, “DGPS High Accuracy Velocity Determination Using Doppler Measurements”, *Proceedings of the International Symposium on Kinematic Systems (KIS) 97*, Banff, Canada, 3-6 June 1997.

11. S. Moafipoor, D.A. Grejner-Brzezinska and C.K. Toth, “Tightly Couple GPS/INS Integration Based On GPS Carrier Phase Velocity Update”, *Proceedings of ION 2004 National Technical Meeting*, San Diego, California, 26-28 January, 2004.

12. J. Wendel and G.F. Trommer, “Tightly Coupled GPS/INS In tegration for Missle Applications”, *Journal of Aerospace Sc ience and Technology*, No. 8, 2004.

13. H. K. Lee, J. G. Lee, C. G. Park, and Y. K. Rho, " Modeling Quaternion Errors in SDINS: Computer Fram e Approach", *IEEE Transactions on Aerospace and Ele ctronic Systems*, Vol. 34, No. 1, 1998.

14. H. K. Lee, J. G. Lee, and G. I. Jee, “GPS Multipath Detection Based on Successive-Time Double-Difference s”, *IEEE Signal Processing Letters, Vol. 11*, No. 3, 20 04.

15. H. K. Lee, C. Rizos, and G. I. Jee, "Design of Kinem atic DGPS Filters with Consistent Error Covariance Inf ormation", *IEE Proceedings - Radar, Sonar and Navig ation*, Vol. 151, No. 6, 2004.